The contribution of black carbon to global ice nucleating particle concentrations relevant to mixed-phase clouds

Gregory P. Schill[a,1,2], Paul J. DeMott[a], Ethan W. Emerson[b], Anne Marie C. Rauker[b,3], John K. Kodros[a,4], Kaitlyn J. Suski[a,5], Thomas C. J. Hill[a], Ezra J. T. Levin[a], Jeffrey R. Pierce[a], Delphine K. Farmer[b], and Sonia M. Kreidenweis[a]

[a]Department of Atmospheric Science, Colorado State University, Fort Collins, CO 80523-1371; and [b]Department of Chemistry, Colorado State University, Fort Collins, CO 80523-1872

Edited by Steven C. Wofsy, Harvard University, Cambridge, MA, and approved July 28, 2020 (received for review January 29, 2020)

Black carbon (BC) aerosol plays an important role in the Earth's climate system because it absorbs solar radiation and therefore potentially warms the climate; however, BC can also act as a seed for cloud particles, which may offset much of its warming potential. If BC acts as an ice nucleating particle (INP), BC could affect the lifetime, albedo, and radiative properties of clouds containing both supercooled liquid water droplets and ice particles (mixed-phase clouds). Over 40% of global BC emissions are from biomass burning; however, the ability of biomass burning BC to act as an INP in mixed-phase cloud conditions is almost entirely unconstrained. To provide these observational constraints, we measured the contribution of BC to INP concentrations ([INP]) in real-world prescribed burns and wildfires. We found that BC contributes, at most, 10% to [INP] during these burns. From this, we developed a parameterization for biomass burning BC and combined it with a BC parameterization previously used for fossil fuel emissions. Applying these parameterizations to global model output, we find that the contribution of BC to potential [INP] relevant to mixed-phase clouds is ∼5% on a global average.

ice nucleation | biomass burning | mixed-phase clouds | black carbon | chemical transport model

Black carbon (BC) is the primary light-absorbing aerosol in the atmosphere. Its short lifetime (days to weeks) relative to CO_2 and methane makes it an intriguing target for near-term climate mitigation (1). Errors associated with BC climate forcing, however, obfuscate its efficacy as a climate mitigator. The largest contributions to BC's forcing uncertainties are often attributed to its effects on clouds, in particular mixed-phase clouds [i.e., clouds containing supercooled cloud droplets and ice particles, (2)]. Efforts to reduce these uncertainties are hindered by the complexity of aerosol–cloud interactions (3). Particularly vexing is quantifying the abundance and identity of ice nucleating particles (INPs). INPs provide the only pathway for primary ice formation in mixed-phase clouds; however, they are rare [e.g., ∼1 in 10^6 particles are INPs at −20 °C (4)]. Despite their rarity, INPs influence mixed-phase cloud ice concentrations and precipitation and therefore alter cloud albedo and lifetime (5). Furthermore, the INP properties of aerosols, such as BC, will affect their own lifetime, vertical structure, and transport to climate-sensitive regions such as the Arctic (6). Despite its importance to the Earth's climate and near-term climate mitigation strategies, the INP efficiency of BC relevant to mixed-phase clouds remains almost entirely unconstrained from direct observations, encumbering attempts to estimate BC's impact on mixed-phase clouds in modeling studies (7).

BC's efficacy as an immersion-freezing INP (henceforth, INP will refer only to freezing by particles encapsulated within supercooled cloud droplets, termed immersion freezing and pertinent to mixed-phase cloud conditions) has been studied in the laboratory for decades, with starkly conflicting results. Early laboratory studies showed that acetylene and kerosene flame-generated soot can nucleate ice below −20 °C. (8, 9); after normalizing for surface area, these studies indicated that BC may be more ice active than the well-known INP mineral dust (10). Results from later laboratory studies were contradictory, suggesting that BC was not active as an INP above instrument limits of detection. These included soot aerosols from miniCAST soot generators, graphite spark generator soot, hydrocarbon flame-generated soot, and fullerene soot, as well as various lamp blacks and carbon blacks (11–15).

Unfortunately, field study measurements of the contribution of BC to INP concentrations ([INP]) have also been inconclusive. For example, in-cloud measurements from the high-altitude observatory at Jungfraujoch, Switzerland saw that BC is enriched in ice-particle residuals and therefore may efficiently nucleate ice

Significance

The Earth's climate is affected by the radiative properties of clouds. In clouds containing both supercooled water droplets and ice particles (mixed-phase clouds), cloud lifetime and albedo are affected by the presence of ice nucleating particles (INP). After decades of research, the importance of black carbon (BC) as an INP remains unresolved. In this work, we determined the contribution of BC to INP concentrations ([INP]) from real-world wildfires and prescribed burns. We found that BC does not contribute significantly to [INP] in near-field biomass burning plumes. These results were applied as parameterizations to global climate model output. Combined with previous work on diesel-engine exhaust, we find that BC does not contribute significantly to global [INP] relevant to mixed-phase clouds.

Author contributions: G.P.S., P.J.D., and S.M.K. designed research; G.P.S., E.W.E., A.M.C.R., J.K.K., K.J.S., T.C.J.H., and E.J.T.L. performed research; G.P.S., P.J.D., J.R.P., D.K.F., and S.M.K. contributed new reagents/analytic tools; G.P.S., A.M.C.R., J.K.K., and T.C.J.H. analyzed data; and G.P.S. wrote the paper.

The authors declare no competing interest.

This article is a PNAS Direct Submission.

[1]Present addresses: Cooperative Institute for Research in Environmental Sciences, University of Colorado, Boulder, CO 80309; and Chemical Sciences Laboratory, National Oceanic and Atmospheric Administration, Boulder, CO 80305.

[2]To whom correspondence may be addressed. Email: gregory.schill@noaa.gov.

[3]Present address: O'Neill School of Public and Environmental Affairs, Indiana University, Bloomington, IN 47405.

[4]Present address: Institute of Chemical Engineering Sciences (ICE-HT), Foundation for Research and Technology Hellas (FORTH), GR-26504 Patras, Greece.

[5]Present address: Research and Development, JUUL Labs, San Francisco, CA 94107.

This article contains supporting information online at https://www.pnas.org/lookup/suppl/doi:10.1073/pnas.2001674117/-/DCSupplemental.

First published August 24, 2020.

(16); later measurements at the same site, however, saw that BC is depleted in the ice phase, which suggests that BC does not play a significant role in mixed-phase cloud ice nucleation (17, 18).

These contradictions in laboratory and field studies suggest that fuel type and combustion conditions determine the ice nucleation properties of BC. Such conditions prescribe BC's physical and morphological properties as well as its coemitted and coagulated species. Major BC fuel types include fossil fuels and flammable biomass, and major combustion sources include diesel exhaust, residential fuel burning, prescribed burns, and wildfires (2). BC particles from fossil fuel combustion and anthropogenic pollution are not significant sources of INPs. For example, studies on diesel exhaust have shown that less than 1 in 10^9 BC particles are ice nucleation active at -30 °C (19). Furthermore, ambient [INP] in Beijing, China were relatively constant over several weeks despite BC concentrations varying by a factor of 30 and reaching values as high as 17.26 $\mu g \cdot m^{-3}$ (20).

Elevated [INP] have been observed in biomass-burning smoke during laboratory and field studies (21–23); however, it is unclear from these studies if the INPs are actually BC. Some studies have shown that BC may be the dominant INP type in select biomass burning conditions. For example, soot particles were found to contribute up to 64% of the INPs in prescribed burns within a predominantly wiregrass understory (24). Furthermore, BC contributed up to 70% to [INP] in controlled laboratory burns of grasses (25). As biomass burning represents ∼40% of global BC emissions (2), BC from biomass burning could be a significant source of INP globally. In both of these studies, however, the overall ice-active fractions may be too low to influence [INP], even on the regional level (21). Thus, it remains unclear whether BC contributes to [INP] outside of thick plumes and on a global scale (26).

Regional- and global-scale estimates of BC [INP] rely on models that can implement theory-based or empirical ice nucleation parameterizations. Using parameterizations based on BC INP activity from the acetylene and kerosene-burner soot studies, models have found that BC contributes ∼50% to [INP] in springtime low-level Arctic mixed-phase clouds (27), and 23 to 61% to global [INP] depending on dust loadings (28). Taking into account the aforementioned negative results, these modeling studies highlight that BC's contribution to [INP] is poorly constrained and is estimated to vary from no contribution to being the most abundant INP globally.

To assess the role of BC from biomass burning as an INP, we determined the contribution of refractory BC (rBC)-containing particles to [INP] from field measurements of both prescribed burns and wildfires using the single-particle soot photometer coupled to a continuous-flow diffusion chamber (SP2-CFDC) (29, 30). The SP2-CFDC selectively removes rBC from an aerosol stream and quantifies that effect on [INP]. From these burns, we found that rBC-containing particles contributed $\leq$10% to [INP]. From these results, we developed a surface-area normalized parameterization for BC INPs from biomass burning. The parameterization aligns well with other surface-area normalized parameterizations derived from laboratory proxies of BC and diesel exhaust BC (15, 19, 31). These parameterizations are over four orders of magnitude lower than the parameterization derived from acetylene and kerosene-burner soot studies and used in the aforementioned modeling studies. Assuming the INP characteristics of BC from the burns in this study can be extended to different biomass-burning fuel types and combustion conditions, this study strongly suggests that BC is not an efficient INP. Under this assumption, we assessed the global importance of BC as an INP by applying our parameterization to simulated biomass-burning aerosol from a global chemical transport model. A similar parameterization for diesel exhaust (19) was applied to simulated fossil fuel BC. From these treatments, we estimate that BC's contribution to simulated, potential [INP] is only ∼5% on a global average.

Results and Discussion

The Contribution of rBC-Containing Particles to [INP] in Near-Field Prescribed Burns and Wildfires. To determine the contribution of rBC-containing particles to [INP] during biomass burning events, we measured [INP] using the SP2-CFDC. The SP2-CFDC directly determines the contribution of rBC-containing particles to [INP] by selectively filtering out rBC-containing particles from an aerosol stream (29). Filtering occurs within the SP2, where a 1,064-nm laser heats rBC to its vaporization temperature (∼4,000 K) (30). During vaporization, ice nucleating entities present in a nonrefractory coating will also be vaporized. Refractory INPs, such as mineral dust, that are partially attached to rBC may have their ice nucleation potential altered, but not with uniform efficiency (29, 30). rBC-containing contributions to [INP] are derived by toggling the SP2 laser on and off and taking the ratio of adjacent SP2 laser-on and laser-off periods. Thus, by definition, the rBC-containing contributions can be negative; negative values are kept for averaging, as omitting them would introduce a positive bias.

Using the SP2-CFDC, we sampled smoke from several western US wildfires and grassland prescribed burns (*SI Appendix*, Table S1). A representative time series from one sampling period during the Pioneer Wildfire (August 2016; 32 miles northeast of Boise, ID) can be seen in Fig. 1*A*. Roadside measurements were taken in the Colorado State University (CSU) mobile laboratory, and smoke was sampled from an inlet on the roof ∼5 m above ground level. During the first 3 h, a capping inversion kept aerosol concentrations both high and relatively stable, with total aerosol concentrations above 2×10^4 cm^{-3} and rBC concentrations above 1,000 cm^{-3}. A combination of high and stable rBC loadings represents near-perfect sampling conditions for the SP2-CFDC. The average and median SP2-laser-off [INP] at -30 °C ($[INP]_{-30\,°C}$) were 92 and 76 L^{-1}, respectively. These concentrations are elevated in comparison to unperturbed continental landscapes (24, 32, 33), which suggests that INPs are sourced from the fire. When the SP2 laser was on, the concentration of particles with diameters greater than 500 nm (n500, from CFDC optical particle counter) decreased by 18 ± 2% (Fig. 1*A*). This is evident in both the 1-Hz data (sticks) and 3- to 5-min averages (markers). Similar behavior in $[INP]_{-30\,°C}$, however, was not observed; the SP2-laser-on $[INP]_{-30\,°C}$ decreased by 0 ± 30%. Thus, on average, BC did not contribute to $[INP]_{-30\,°C}$ despite rBC concentrations being >1,000 cm^{-3}. At ∼12:00 PM Mountain Standard Time (MST), the capping inversion lifted and the total aerosol concentrations, rBC concentrations, n500, and $[INP]_{-30\,°C}$ all dropped by an order of magnitude or more, confirming that INPs were sourced from biomass burning.

The rBC contribution to n500 and [INP] for all wildfires and prescribed burns in this study are similar to those in the Pioneer Wildfire (Fig. 2). For both wildfires and prescribed burns, rBC-containing particles contribute 12 to 19% (interquartile range [IQR]) to n500. rBC cores larger than 500 nm are only 1% of n500; thus most of the rBC-containing particles with diameters >500 nm are rBC cores coated with nonrefractory material. In contrast to n500 contributions, the contribution of rBC-containing particles to [INP] is either zero or within one SD of zero. These results are similar across all fires despite sampling both near-field and transported smoke, as well as a diversity of major fuel types (*SI Appendix*, Table S1). Across all sampling periods, rBC's contribution to [INP] was −8 to 7% (IQR), with a median value of 3% and a mean of 1%. Normalizing to give equal weight to each fire, the average contribution of rBC to [INP] across all fires was 4%, with the largest fire-averaged contribution being 10%.

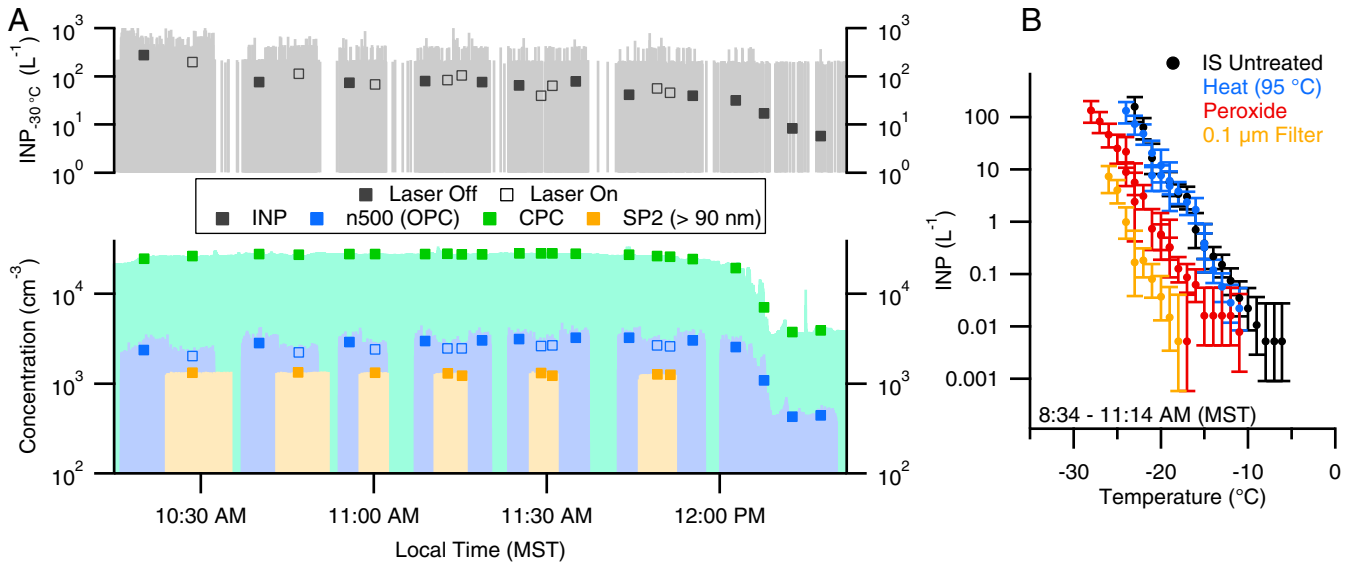

Fig. 1. (*A* and *B*) A representative time series (*A*) and corresponding IS INP temperature spectra (*B*) from the Pioneer Wildfire (22 August 2016). In the time series, INP concentration at −30 °C ($[INP]_{-30\,°C}$), the number of particles with diameters >500 nm (n500), rBC number concentrations from the single-particle soot photometer (SP2), and total particle number concentrations from a condensation particle counter (CPC) are shown as 1-Hz data (sticks) and 3- to 5-min averages (markers). For $[INP]_{-30\,°C}$ and n500, open and solid markers represent times when the SP2 was laser on and off, respectively. The IS INP temperature spectra are from the same day (MST times in the bottom left-hand corner) and show the effect of pretreatments with heat, peroxide, and size exclusion of particles >0.1 μm.

In addition to the SP2-CFDC, we also collected aerosol on filters for offline INP analysis. Offline techniques are disadvantageous because they have poor time resolution and particles must be rinsed off the filters and collected in bulk water; however, filters can collect more particles than online methods and thus allow measurement at warmer temperatures when [INP] may be below the CFDC's limit of detection. Furthermore, bulk water from rinsed filters can be treated with heat, hydrogen peroxide, and size exclusion methods to assess the importance of biological particles, organics, and size, respectively (33).

Offline INP analysis using the ice spectrometer (IS) (34) corroborates that BC is not significantly contributing to [INP] from wildfires and prescribed burns. The IS temperature spectrum for a filter collected during the Pioneer Wildfire can be seen in Fig. 1*B*. At T > −15 °C, heat-labile INPs account for 51% of the [INP] in this plume and 62 to 90% (IQR) in all plumes (*SI Appendix*, Fig. S1). At T ≤ −15 °C, however, heat had little effect on the ice nucleation activity of biomass-burning aerosol. This suggests that heat-labile organics, such as proteins or other biological particles, do not contribute appreciably to [INP] at these temperatures. Treatment with both heat and peroxide does reduce [INP] at T ≤ −15 °C by ∼94%. The heat-plus-peroxide treatment has been used in the past to determine the contribution of all organic material to INPs (32). Size exclusion measurements showed that the INPs are larger than 100 nm (Fig. 1*B*); thus, these organics are likely not water-soluble macromolecules (35). As BC is unaffected by heat-and-peroxide digestion (36), its maximum contribution to [INP] is 6% in this fire. We find similar results for all near-field smoke plumes, with heat-resistant organics contributing 88 ± 8% (prescribed burns) and 95 ± 2% (wildfire smoke) to [INP] at T ≤ −15 °C (*SI Appendix*, Fig. S1). Thus, from offline measurements, the maximum contribution of rBC to [INP] is ∼12% for prescribed burn and ∼5% for wildfires. These estimates are maximum contributions as other heat-and-peroxide–resistant ice nucleating entities, such as the mineral component of dust, can also be contributing.

Unfortunately, the techniques used in this study cannot directly determine the identity of these insoluble, organic INPs. We hypothesize that they may be organics bound to lofted soil dust particles or insoluble organic particles such as tar balls (37). Soil-dust aerosols have been observed in western US wildfires (38), as well as in fresh prescribed burns (39), and have been previously shown to be efficient INPs (32). Furthermore, organic INPs such as tar balls and other carbonaceous particles have been directly observed in CFDC ice-crystal residuals from two separate western US wildfires (24). Finally, it is unclear how important these organic INPs are for different fuel types and biomes beyond the fires in this study. This suggests that more measurements of INPs from biomass burning are needed, particularly as these insoluble,

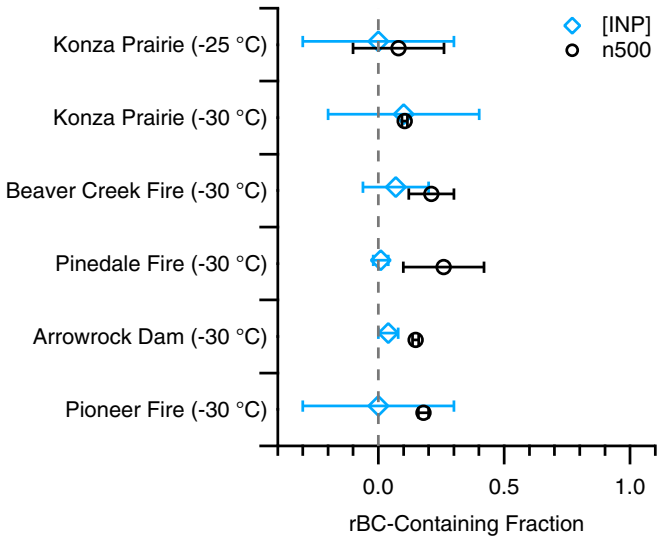

Fig. 2. The average and SD of the contribution of rBC-containing particles to ice [INP] and the number of particles >500 nm in diameter (n500). Both [INP] and n500 contributions are averaged over an entire fire, consisting of 4 to 8 h of sampling time each.

organic INPs do not have parameterizations for implementation in models.

Updated INP Parameterization. Ice nucleation in global climate models is generally parameterized due to computational expense. One parameterization framework, the singular hypothesis, stipulates that the time dependence of immersion freezing is of secondary importance to temperature (40). Thus, the ice nucleation active surface site density (n_s) can be described as a function of temperature only:

$$n_s(T) = \frac{ln(1 - AF(T))}{SA_{aerosol}}. \quad [1]$$

Here, AF is the number fraction of aerosol active as INPs at temperature T, and $SA_{aerosol}$ is the surface area per aerosol particle. Using the SP2-CFDC, we estimate a BC-specific n_s parameterization for biomass burning. To do so, we assume that 4% (range 1 to 10%) of the measured INPs are rBC (INP_{rBC}). Dividing INP_{rBC} by the total number of rBC particles renders AF_{rBC}. The mass per particle is determined by dividing the rBC mass concentration by the rBC number concentrations, and $SA_{aerosol}$ is estimated by applying a specific surface area [70 m^2 g^{-1}, mini-CAST brown, (15)] to the mass per particle.

The calculated n_s values for rBC in prescribed burns and wildfires cluster around several limit-of-detection parameterizations derived from proxies of atmospheric BC (13, 19, 31) (Fig. 3). This is verified from both the IS and CFDC measurements. The biomass-burning rBC n_s values are over four orders of magnitude lower than estimates using only the acetylene- and kerosene-generated soot. Thus, although these n_s values are for rBC from real-world biomass burning, they are consistent with previous laboratory proxies of BC and BC from diesel engine exhaust, suggesting that BC is not an efficient INP regardless of combustion source.

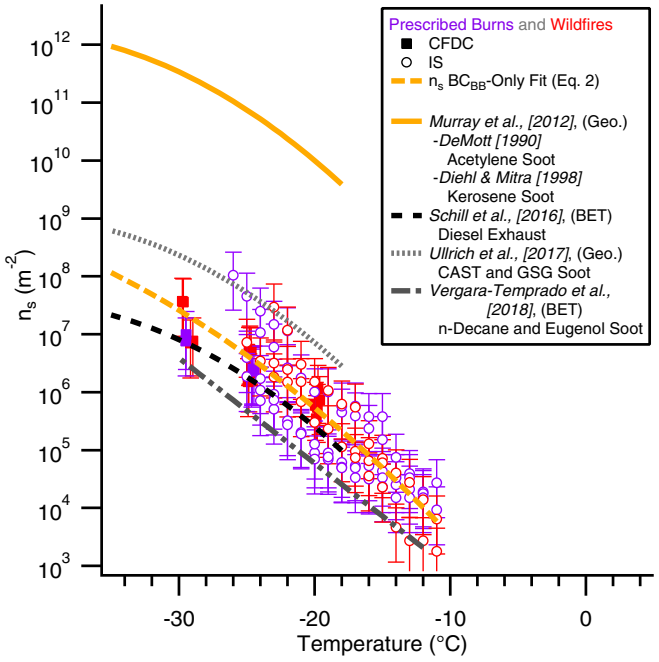

Fig. 3. Ice nucleation active surface site densities (n_s) for BC as a function of temperature. Markers indicate values from this work, while lines are limit-of-detection parameterizations from both this work and previous works (8–10, 13, 14, 19). The method of surface-area normalization (BET or geometric [Geo.]) is indicated in the key. Error bars correspond to a range of BC contributions to ice nucleating particle concentrations (1 to 10%).

Laboratory burns during the Fourth Fire Laboratory at Missoula Experiments (FLAME-4) and prescribed burns in the southeastern United States have shown that BC-containing particles can make up a majority of the biomass-burning INPs (24, 25). These results seem to contradict the results presented here; however, BC INPs in those burns were not significantly more abundant when normalizing for total aerosol (*SI Appendix*, Table S2). Thus, in those studies, BC INPs made up a higher fraction of the total [INP] because other, non-BC INPs were less abundant. Furthermore, assuming similar BC-to-total-aerosol number ratios and SA_{BC}, the n_s values from FLAME-4 and southeastern United States prescribed burns would cluster around the markers in Fig. 3.

Atmospheric Implications

To determine the global importance of BC INPs, we derived [INP] by using n_s parameterizations for each aerosol type and simulating aerosol number and surface area concentrations using the chemical transport model GEOS-Chem, version 10.01 (http://www.geos-chem.org). With n_s (T), number concentrations, and surface area concentrations, we can derive [INP] for each particle type by rearranging Eq. **1**. Simulated INPs are derived from model aerosol output. Aerosols in the model do not affect the cloud fields, but are affected by clouds through wet removal and aqueous oxidation. Thus, in this work, simulated INPs are not particles that have been activated into ice crystals and removed via ice-initiated precipitation; rather, they are aerosols that could potentially be INPs if they were activated into a cloud droplet and cooled to a prescribed temperature. Thus, henceforth, we use the term "potential [INP]" to describe simulated [INP] calculated from n_s parameterizations. Specifically, we used the following n_s parameterization for simulated biomass-burning BC:

$$n_s\,(-36 \le T \le -11\,^{\circ}\mathrm{C}) = exp(1.844 - 0.687 \times T - 0.00597 \times T^2). \quad [2]$$

A diesel exhaust parameterization (19) was used for simulated fossil fuel BC. Thus, these results assume that the INP properties of all biomass-burning BC are similar to the those of the burns in this study and that all fossil fuel BC has similar INP properties to diesel exhaust. We then compared potential BC [INP] to potential dust and sea-spray [INP]. Simulated potential dust INPs were derived using the Niemand et al. (41) parameterization (N12) and potential marine-organic INPs were accounted for by applying a pristine marine aerosol parameterization (42) to modeled sea-spray aerosol.

To assess the model's skill at simulating INPs, we compared potential [INP] to a compilation of observations from eight different field studies (*SI Appendix*, Fig. S2). The studies were chosen to represent background conditions over the open ocean, at coastal sites, and over continental sites. We also included one study that sampled Saharan dust plumes during the Ice in Clouds Experiment–Dust (ICE-D) (43). The model outputs gridded and monthly averaged aerosol concentrations; thus, the observed [INP] during ICE-D, which targeted episodic dust plumes, are not expected to compare well with the simulated, potential [INP]. Nonetheless, we include it here for bounding purposes. Simulated [INP] were matched to the observed [INP] by latitude, longitude, month, temperature, and pressure altitude. Most of the observed [INP] were taken near ground level. In general, the model tends to overestimate [INP] compared to the observations (*SI Appendix*, Fig. S3*A*). It has been noted previously that N12, which was predicated upon laboratory studies, may overpredict [INP] in air containing appreciable loadings of atmospheric dust (31, 43). Thus, we have scaled N12 to observations during ICE-D where the dust surface area loading was high

($N12_{scaled}$; *SI Appendix*, Fig. S4). When applying $N12_{scaled}$, we used the original N12 temperature bounds ($-36 \leq T \leq -12$ °C). Using $N12_{scaled}$ (equation in key in *SI Appendix*, Fig. S4), over 75% of the model predictions were within one order of magnitude of the observations (*SI Appendix*, Fig. S3*B*).

Even when using $N12_{scaled}$, the model overestimates [INP] during the ARM Cloud Aerosol Precipitation Experiment (ACAPEX) by a factor of 100 (*SI Appendix*, Fig. S3*B*). The model suggests that 98% of the potential INPs are dust; however, aircraft measurements during ACAPEX suggest that dust is not the dominant INP type (4). Thus, in addition to the n_s parameterizations, aerosol transport and removal mechanisms in the model are additional sources of uncertainty in potential [INP]. An exploration of these additional biases requires further validation that is beyond the scope of this work.

Simulated, potential [INP] in GEOS-Chem suggest that BC is not an important contributor to potential [INP] globally. At the 850-hPa pressure level (~1.5 km in altitude), potential BC [INP] active at −20 °C ($[INP]_{-20°C}$) are dominant only over continental South America, southern Africa, and parts of Canada and Indonesia (Fig. 4). BC emissions in these regions are dominated by biomass burning. In this study, organic INPs were >10 times more abundant than BC INPs in fresh biomass-burning plumes. Thus, these results suggest that BC or organic INPs may contribute significantly to $[INP]_{-20°C}$ regionally. Globally and at low altitudes, dust dominates potential $[INP]_{-20°C}$ over much of the Northern Hemisphere and sea spray does the same in the Southern Hemisphere high latitudes. The average contribution of BC to potential $[INP]_{-20°C}$ at 850 hPa, normalized to each model grid box, is only 4% (96% biomass burning and 4% fossil fuel); however, this percentage will be influenced in some regions by overestimations in dust loadings.

To assess the altitude dependence of potential [INP], we can use the model's monthly averaged ambient temperature up to −12 °C to calculate [INP] ($[INP]_{ambient}$; *SI Appendix*, Fig. S5). Here, the picture remains largely the same as Fig. 4. At temperatures sufficiently cold to activate ice, sea spray dominates potential $[INP]_{ambient}$ in the Southern Hemisphere high latitudes and dust dominates the entire Northern Hemisphere. Simulated BC INPs contribute significantly to potential $[INP]_{ambient}$ only at high altitudes in the Southern Hemisphere tropics and midlatitudes, amounting to a globally averaged BC contribution to potential $[INP]_{ambient}$ of 6% (91% biomass burning and 9% fossil fuel). Thus, we can conclude, from parameterizations based on the direct contribution of BC to INPs from real-world carbonaceous combustion sources, that BC is not a significant contributor to global, potential [INP] impacting mixed-phase clouds.

Conclusions

In this work, we have directly measured the contribution of BC to [INP] from real-world prescribed burns and wildfires using the SP2-CFDC (29, 30). We found that, on average, BC contributes ~4% to INP emissions from biomass burning and was always ≤10% for a single fire. Using SP2 number and mass concentrations, we developed a number-and-surface-area normalized INP parameterization for BC from biomass burning. Combined with a similar parameterization for BC from fossil fuel combustion (19), we find that BC contributes ~5% to simulated, potential [INP] on a global, annual average. Thus, BC is likely a minor contributor to global [INP] relevant to mixed-phase clouds. Our findings help to constrain the indirect radiative forcing attributable to BC and, in particular, suggest that the assumed biomass-burning BC INP activity in previous parameterizations should undergo downward revisions.

Materials and Methods

Sampling near-field to prescribed burns and wildfires required a mobile sampling platform, oftentimes using gasoline generators to power instruments. Due to power limitations of the generators, we sampled with a limited aerosol package—using only the SP2-CFDC, a TSI 3776 condensation particle counter, and dual-chamber diaphragm pumps for the filter collection.

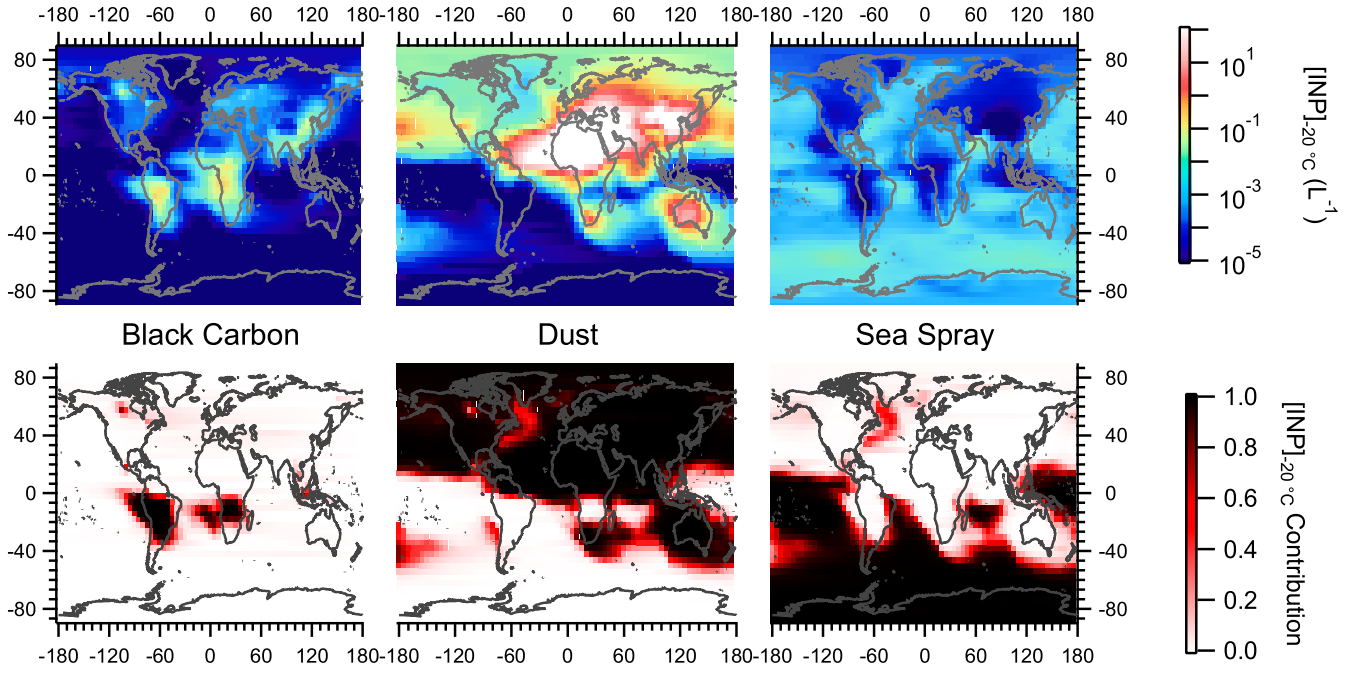

Fig. 4. Annually averaged potential [INP] at −20 °C ($[INP]_{-20\,°C}$) at 850 hPa for BC, dust, and sea spray (*Top Row*) and the ratio of each species potential $[INP]_{-20\,°C}$ to the potential $[INP]_{-20\,°C}$ from all species summed together (*Bottom Row*).

CSU Mobile Laboratory. The CSU mobile laboratory consists of a custom-designed vehicle (Brown Specialty Vehicles) with an 8′ high × 8′ wide × 14′ long aluminum body. An aerosol inlet, used for online instrumentation, was attached to a sampling port on the roof of the mobile laboratory. In addition to ground power, the mobile laboratory can be powered by generators (Honda RU6500is, EU3000i), which allow for sampling in more remote locations. Sampling locations were chosen to be downwind of biomass-burning events, but also to minimize BC influence from road traffic. Gasoline generators do not emit BC aerosol; however, they were also placed downwind of the mobile laboratory to reduce influence from gas-phase constituents.

SP2-CFDC. The SP2-CFDC, its operation principles, and its limitations have all been addressed in detail (29, 30). Briefly, we have modified the SP2 so that the CFDC can sample from its exhaust without contamination. Under normal operation, the SP2 detects particles via laser-induced incandescence (LII) by a 1,064-nm continuous-wave laser. During LII, BC particles absorb enough laser energy to heat to their vaporization temperature (∼4,000 K). Under the right SP2 conditions [power ≥930 nW/(220-nm polystyrene latex sphere)], rBC and its nonrefractory coatings are fully vaporized. Since BC is the dominant atmospheric aerosol that absorbs 1,064-nm light, the SP2 acts a prefilter to selectively remove rBC-containing particles from an aerosol stream entering the CFDC. By toggling the SP2 laser on and off, the contribution of rBC-containing particles to [INP] can be measured from stable aerosol concentrations.

The CFDC itself has also been detailed in previous works (44), and thus only its general principle is described here. The CSU CFDC is a vertically oriented thermal gradient diffusion chamber. In the upper two-thirds of the CFDC, an aerosol stream is subjected to water-supersaturated conditions [typically water relative humidity (RH_{water}) = 105%] and subzero temperatures (typically ≤ -15 °C). Here particles activate into supercooled liquid drops and, if they contain ice nucleating entities active at the set temperature, nucleate ice. In the lower third of the CFDC, the temperature is colder and the RH is held at ice supersaturation. Under these conditions, the droplets evaporate, but ice particles persist. Particles are detected at the bottom of the CFDC using a calibrated optical particle counter. An ice threshold is operationally defined, usually >3 μm. At the CFDC inlet, a 2.5-μm impactor removes particles that would be confounded as ice.

IS. The CSU IS is an offline technique, which has the advantage of measuring at warmer temperatures, because of its lower detection limit of ∼0.001 $INP{\cdot}L^{-1}$ (4, 33, 34). In principle, INPs are suspended in deionized (DI) water, dispersed as 50-μL aliquots into 96-well PCR trays placed into Al blocks, and cooled using a chiller bath. In this work, we collected aerosol onto precleaned 0.2-μm Nuclepore filters, which were held in open-faced Nalgene filter units (33). A dual-chamber diaphragm pump pulled ∼10 liters per minute across the face of the filter. Filters were rinsed of INPs by placing them in a 50-mL Falcon polypropylene tube with 8 to 10 mL of DI water and shaken end over end for 20 min. Generally, each IS run consisted of 1) an undiluted sample; 2) 20-, 400-, and 8,000-fold dilutions in DI water; and 3) a handling blank that undergoes the same treatment as the sample filter.

Treatments of the filter-rinse water by heat, peroxide, and size exclusion have also been described in detail previously (33). Briefly, heat treatment involves heating the filter-rinse water to 95 °C for 20 min and is useful for denaturing proteins and other heat-labile biological nanoparticles. The peroxide treatment also involves heating to 95 °C for 20 min, but adds H_2O_2 to a final concentration of 10% and illuminates that solution with ultraviolet B light to generate hydroxyl radicals. This destructively oxidizes all organic species. Finally, size exclusion involves passing rinse water through a syringe filter to exclude particles with diameters >0.1 or 0.2 μm. The filtrate is then tested for INPs.

GEOS-Chem and Applying n_s Parameterizations. To simulate global-scale BC, sea-spray, and dust concentrations, as well as other aerosol species, we used the global chemical transport model GEOS-Chem version 10.01 (http://www.geos-chem.org). We simulated the year 2010 with 1 mo of model spin-up at 4° × 5° horizontal resolution and 47 vertical layers. The model year 2010 was used to directly compare to previous works (19) and because model runs from 2010 have been validated against observations of particle size distributions (45). The model was driven by the Goddard Earth Observing System, Version 5 assimilated meteorology fields. Fossil fuel and biofuel emissions are from Bond et al. (46), and biomass-burning emissions are from the Global Fire Emissions Database version 3 (47). Biomass-burning mass concentrations were calculated from a fossil fuel emissions on vs. off approach. Sea-spray emissions follow the scheme of Jaeglé et al. (48), and dust emissions are based on the DEAD scheme (49).

In this work, a one-moment aerosol scheme was used. Particle number concentrations were calculated from particle mass concentrations by assuming lognormal distributions with one mode (for BC), two modes (for sea spray), or three modes (for dust) (45). Simulated aerosols are externally mixed; however, the INPs in this work are primary particles. In the model, the assumed size distributions are representative of aged particles and account for coagulation within a single particle type (e.g., BC coagulation near sources), but do not account for coagulation between primary particle populations (e.g., BC mixing with dust). We believe that coagulation between primary particle populations is likely small on a global scale. Thus, the assumption of externally mixed aerosols likely has little impact on predictions of INPs in this work. Surface areas were either derived directly from mass concentrations using Brunauer–Emmett–Teller surface areas (for BC) or calculated assuming the particles were spheres of a prescribed density (for sea spray and dust). Different BET surface areas were used for fossil fuel BC [108 $m^2{\cdot}g^{-1}$ (19)] and biomass-burning BC [70 $m^2{\cdot}g^{-1}$ (15)]. The density of sea salt and dust, as well as the median diameters and geometric standard deviations used in the lognormal distributions, can be found in Kodros and Pierce (45).

Data Availability. For each figure in this paper, a data file, a metadata file, and code to recreate the figure in Igor Pro (version 8.04) have been deposited in an online repository at the University of Colorado (https://scholar.colorado.edu/concern/datasets/8w32r669m).

ACKNOWLEDGMENTS. G.P.S. was supported by the NSF, Division of Atmospheric and Geospace Sciences Award 1433517. Funding for K.J.S., E.J.T.L., S.M.K., P.J.D., and other logistical support was provided by the NASA, Earth Science Division Award NNX12AH17G. Funding for E.W.E. and D.K.F. is from the Department of Energy, Office of Biological and Environmental Research Award DE-SC0016259.

1. A. P. Grieshop, C. C. O. Reynolds, M. Kandlikar, H. Dowlatabadi, A black-carbon mitigation wedge. *Nat. Geosci.* **2**, 533–534 (2009).
2. T. C. Bond *et al.*, Bounding the role of black carbon in the climate system: A scientific assessment. *J. Geophys. Res. Atmos.* **118**, 5380–5552 (2013).
3. H. Morrison *et al.*, Resilience of persistent Arctic mixed-phase clouds. *Nat. Geosci.* **5**, 11–17 (2012).
4. E. J. T. Levin *et al.*, Characteristics of ice nucleating particles in and around California winter storms. *J. Geophys. Res. Atmos.* **124**, 11530–11551 (2019).
5. U. Lohmann, Anthropogenic aerosol influences on mixed-phase clouds. *Curr. Clim. Chang. Reports* **3**, 32–44 (2017).
6. S. M. Fan *et al.*, Inferring ice formation processes from global-scale black carbon profiles observed in the remote atmosphere and model simulations. *J. Geophys. Res. Atmos.* **117**, 1–12 (2012).
7. X. Liu, J. E. Penner, Ice nucleation parameterization for global models. *Meteorol. Z.* **14**, 499–514 (2005).
8. P. J. DeMott, An exploratory study of ice nucleation by soot aerosols. *J. Appl. Meteorol.* **29**, 1072–1079 (1990).
9. K. Diehl, S. K. Mitra, A laboratory study of the effects of a kerosene-burner exhaust on ice nucleation and the evaporation rate of ice crystals. *Atmos. Environ.* **32**, 3145–3151 (1998).
10. B. J. Murray, D. O'Sullivan, J. D. Atkinson, M. E. Webb, Ice nucleation by particles immersed in supercooled cloud droplets. *Chem. Soc. Rev.* **41**, 6519–6554 (2012).
11. M. Dymarska *et al.*, Deposition ice nucleation on soot at temperatures relevant for the lower troposphere. *J. Geophys. Res. Atmos.* **111**, 1–9 (2006).
12. B. Friedman *et al.*, Ice nucleation and droplet formation by bare and coated soot particles. *J. Geophys. Res. Atmos.* **116**, 1–11 (2011).
13. R. Ullrich *et al.*, A new ice nucleation active site parameterization for desert dust and soot. *J. Atmos. Sci.* **74**, 699–717 (2017).
14. J. Vergara-Temprado *et al.*, Is black carbon an unimportant ice-nucleating particle in mixed-phase clouds? *J. Geophys. Res. Atmos.* **123**, 4273–4283 (2018).
15. F. Mahrt *et al.*, Ice nucleation abilities of soot particles determined with the Horizontal Ice Nucleation Chamber. *Atmos. Chem. Phys.* **18**, 13363–13392 (2018).
16. J. Cozic *et al.*, Black carbon enrichment in atmospheric ice particle residuals observed in lower tropospheric mixed phase clouds. *J. Geophys. Res. Atmos.* **113**, 1–11 (2008).
17. M. Kamphus *et al.*, Chemical composition of ambient aerosol, ice residues and cloud droplet residues in mixed-phase clouds: Single particle analysis during the cloud and aerosol characterization experiment (CLACE 6). *Atmos. Chem. Phys.* **10**, 8077–8095 (2010).
18. P. Kupiszewski *et al.*, Ice residual properties in mixed-phase clouds at the high-alpine Jungfraujoch site. *J. Geophys. Res.* **121**, 12343–12362 (2016).
19. G. P. Schill *et al.*, Ice-nucleating particle emissions from photochemically aged diesel and biodiesel exhaust. *Geophys. Res. Lett.* **43**, 5524–5531 (2016).
20. J. Chen *et al.*, Ice-nucleating particle concentrations unaffected by urban air pollution in Beijing, China. *Atmos. Chem. Phys.* **18**, 3523–3539 (2018).

21. M. D. Petters *et al.*, Ice nuclei emissions from biomass burning. *J. Geophys. Res. Atmos.* **114**, 1–10 (2009).
22. A. J. Prenni *et al.*, Biomass burning as a potential source for atmospheric ice nuclei: Western wildfires and prescribed burns. *Geophys. Res. Lett.* **39**, 1–5 (2012).
23. C. H. Twohy *et al.*, Relationships of biomass-burning aerosols to ice in orographic wave clouds. *J. Atmos. Sci.* **67**, 2437–2450 (2010).
24. C. S. McCluskey *et al.*, Characteristics of atmospheric ice nucleating particles associated with biomass burning in the US: Prescribed burns and wildfires. *J. Geophys. Res. Atmos.* **119**, 10458–10470 (2014).
25. E. J. T. Levin *et al.*, Ice-nucleating particle emissions from biomass combustion and the potential importance of soot aerosol. *J. Geophys. Res. Atmos.* **121**, 5888–5903 (2016).
26. V. T. J. Phillips *et al.*, Improvements to an empirical parameterization of heterogeneous ice nucleation and its comparison with observations. *J. Atmos. Sci.* **70**, 378–409 (2013).
27. J. Savre, A. M. L. Ekman, A theory-based parameterization for heterogeneous ice nucleation and implications for the simulation of ice processes in atmospheric models. *J. Geophys. Res.* **120**, 4937–4961 (2015).
28. C. Hoose, J. E. Kristjánsson, J.-P. Chen, A. Hazra, A classical-theory-based parameterization of heterogeneous ice nucleation by mineral dust, soot, and biological particles in a global climate model. *J. Atmos. Sci.* **67**, 2483–2503 (2010).
29. E. J. T. Levin *et al.*, A new method to determine the number concentrations of refractory black carbon ice nucleating particles. *Aerosol. Sci. Technol.* **48**, 1264–1275 (2014).
30. G. P. Schill, P. J. DeMott, J. Ezra, T. Levin, S. M. Kreidenweis, Use of the single particle soot photometer (SP2) as a pre-filter for ice nucleation measurements: Effect of particle mixing state and determination of SP2 conditions to fully vaporize refractory black carbon. *Atmos. Measure. Tech.* **11**, 3007–3020 (2018).
31. B. J. Murray *et al.*, Contribution of feldspar and marine organic aerosols to global ice nucleating particle concentrations. *Atmos. Chem. Phys.* **17**, 3637–3658 (2017).
32. Y. Tobo *et al.*, Organic matter matters for ice nuclei of agricultural soil origin. *Atmos. Chem. Phys.* **14**, 8521–8531 (2014).
33. J. K. Suski *et al.*, Agricultural harvesting emissions of ice-nucleating particles. *Atmos. Chem. Phys.* **18**, 13755–13771 (2018).
34. N. Hiranuma *et al.*, A comprehensive laboratory study on the immersion freezing behavior of illite NX particles: A comparison of 17 ice nucleation.*Atmos. Chem. Phys.* **15**, 2489–2518 (2015).
35. K. Dreischmeier, C. Budke, L. Wiehemeier, T. Kottke, T. Koop, Boreal pollen contain ice-nucleating as well as ice-binding 'antifreeze' polysaccharides. *Sci. Rep.* **7**, 41890 (2017).
36. J. A. Ogren, R. J. Charlson, J. P. Groblicki, Determination of elemental carbon in rainwater. *Anal. Chem.* **55**, 1569–1572 (1983).
37. A. J. Sedlacek *et al.*, Formation and evolution of tar balls from northwestern US wildfires. *Atmos. Chem. Phys.* **18**, 11289–11301 (2018).
38. J. S. Schlosser *et al.*, Analysis of aerosol composition data for western United States wildfires between 2005 and 2015: Dust emissions, chloride depletion, and most enhanced aerosol constituents. *J. Geophys. Res. Atmos.* **122**, 8951–8966 (2017).
39. I. G. Kavouras *et al.*, In situ observations of soil minerals and organic matter in the early phases of prescribed fires. *J. Geophys. Res. Atmos.* **117**, 1–9 (2012).
40. G. Vali, Interpretation of freezing nucleation experiments: Singular and stochastic; sites and surfaces. *Atmos. Chem. Phys.* **14**, 5271–5294 (2014).
41. M. Niemand *et al.*, A particle-surface-area-based parameterization of immersion freezing on desert dust particles. *J. Atmos. Sci.* **69**, 3077–3092 (2012).
42. C. S. McCluskey *et al.*, Marine and terrestrial organic ice-nucleating particles in pristine marine to continentally influenced northeast Atlantic air masses. *J. Geophys. Res. Atmos.* **123**, 6196–6212 (2018).
43. H. C. Price *et al.*, Atmospheric ice-nucleating particles in the dusty tropical Atlantic. *J. Geophys. Res. Atmos.* **123**, 2175–2193 (2018).
44. P. J. Demott *et al.*, Integrating laboratory and field data to quantify the immersion freezing ice nucleation activity of mineral dust particles. *Atmos. Chem. Phys.* **15**, 393–409 (2015).
45. J. K. Kodros, J. R. Pierce, Important global and regional differences in aerosol cloud-albedo effect estimates between simulations with and without prognostic aerosol microphysics. *J. Geophys. Res.* **122**, 4003–4018 (2017).
46. T. C. Bond *et al.*, Historical emissions of black and organic carbon aerosol from energy-related combustion, 1850–2000. *Global Biogeochem. Cycles* **21**, GB2018 (2007).
47. G. R. Van Der Werf *et al.*, Global fire emissions and the contribution of deforestation, savanna, forest, agricultural, and peat fires (1997-2009). *Atmos. Chem. Phys.* **10**, 11707–11735 (2010).
48. L. Jaeglé, P. K. Quinn, T. S. Bates, B. Alexander, J. T. Lin, Global distribution of sea salt aerosols: New constraints from in situ and remote sensing observations. *Atmos. Chem. Phys.* **11**, 3137–3157 (2011).
49. C. S. Zender, H. Bian, D. Newman, Mineral dust entrainment and deposition (DEAD) model: Description and 1990s dust climatology. *J. Geophys. Res. Atmos.* **108**, 4416 (2003).